

NUMERICAL MODELING OF PHASE TRANSFORMATION DURING GRINDING PROCESS

Syed Mushtaq Ahmed Shah^a, M. A. Khattak^{b*}, Muhammad Asad^c, Javed Iqbal^a, Saeed Badshah^d, M. S. Khan^b

^aDepartment of Mechanical Engineering, Balochistan University of Engineering and Technology Khuzdar, Pakistan

^bFaculty of Mechanical Engineering, Universiti Teknologi Malaysia, 81310 UTM Johor Bahru, Johor Malaysia

^cMechanical Engineering department, Prince Muhammad Bin Fahad University, Alkhobar Kingdom of Saudi Arabia

^dDepartment of Mechanical Engineering, International Islamic University Islamabad, Pakistan

Article history

Received

22 February 2017

Received in revised form

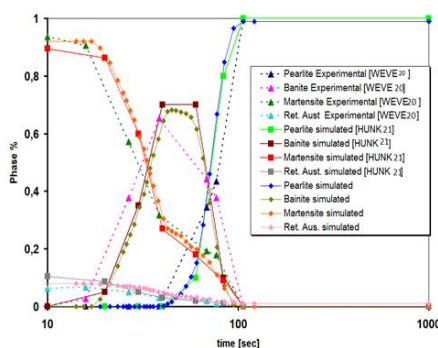
25 April 2017

Accepted

31 May 2017

*Corresponding author
muhdadil@utm.my

Graphical abstract



Abstract

The rapid heating and cooling in a grinding process may cause phase transformations. This will introduce thermal strains and plastic strains simultaneously in a workpiece with substantial residual stresses. The properties of the workpiece material will change when phase transformation occurs. The extent of such change depends on the temperature history experienced and the instantaneous thermal stresses developed. To carry out a reliable residual stress analysis, a comprehensive modelling technique and a sophisticated computational procedure that can accommodate the property change with the metallurgical change of material need to be developed. The objective of this work is to propose a simplified model to predict phase evolution during given temperature history for heating and cooling as encountered during grinding process. The numerical implementation of the proposed model is carried out through the developed FORTRAN subroutine called PHASE using the FEM commercial software Abaqus®/standard. Micro-structural constituents are defined as state variables. They are computed and updated inside the subroutine PHASE. The heating temperature is assumed to be uniform while the cooling characteristics in relation to phase transformations are obtained from the continuous cooling transformation (CCT) diagram of the given material (here AISI 52100 steel). Four metallurgical phases are assumed for the simulations: austenite, pearlite, bainite, and martensite. It was shown that at low cooling rates high percentage of pearlite phase is obtained when the material is heated and cooled to ambient temperature. Bainite is formed usually at medium cooling rates. Similarly at high cooling rates maximum content of martensite may be observed. It is also shown that the continuous cooling transformation kinetics may be described by plotting the transformation temperature, directly against the cooling rate as an alternative to the continuous cooling transformation diagram. The simulated results are also compared with experimental results of Wever [20] and Hunkle [21] and are found to be in a very good agreement. The model may be used for further thermo-mechanical analysis coupled with phase transformation during grinding process.

Keywords: Grinding process, AISI 52100 steel, Phase transformation, numerical modelling, continuous cooling transformation diagram

Abstrak

Pencapaian disebabkan oleh prosesnya yang tidak stabil dan kompleks yang melibatkan pengagihan suhu yang sangat tinggi di zon pencapaian yang boleh memulakan fasa transformasi, berpotensi menjejaskan sisa tegasan dalam sesuatu bahan. Satu model yang telah dipermudahkan untuk meramal fasa evolusi untuk sejarah suhu yang diberikan bagi pemanasan dan penyejukan seperti yang dihadapi semasa proses pencapaian telah dikemukakan. Perlaksanaan berangka untuk model yang dicadangkan telah dijalankan melalui subrutin FORTRAN yang telah dibangunkan yang dipanggil "FASA" menggunakan perisian komersial FEM Abaqus®/piawai. Jujuk mikro-struktur ditakrifkan sebagai pemboleh ubah keadaan. Mereka dihitung dan dikemas kini dalam subrutin FASA. Suhu pemanasan diandaikan sekata manakala ciri-ciri penyejukan berhubung dengan fasa transformasi diperolehi daripada gambar rajah transformasi penyejukan berterusan (CCT) bahan yang diberikan (bagi kes ini keluli AISI 52100). Empat fasa metalurgi diandaikan untuk simulasi ini: austenite, pearlit, bainit dan martensit. Ia juga menunjukkan bahawa kinetik transformasi penyejukan berterusan boleh digambarkan dengan memplot suhu transformasi, secara langsung terhadap kadar penyejukan sebagai alternative kepada gambar rajah CCT. Keputusan simulasi juga dibandingkan dengan keputusan eksperimen oleh beberapa penyelidik dan didapati berada dalam keadaan yang sangat sesuai. Model ini boleh digunakan untuk analisis termo-mekanikal seterusnya ditambah pula dengan fasa transformasi semasa proses pencapaian.

Kata kunci: Proses pencapaian, keluli AISI 52100, fasa transformasi, pemodelan berangka, gambar rajah CCT

© 2017 Penerbit UTM Press. All rights reserved

1.0 INTRODUCTION

Grinding is a commonly used finishing process to produce components of desired shape, size and dimensional accuracy. The ultimate goal in grinding is to have the maximum workpiece quality, minimum machining time and high energetic efficiency. This can be achieved by making a selective adaptation of the possible process strategy and chosen parameter selection. The focus of this study arose from a limitation that challenges the grinding industry. The production rate of ground parts is generally constrained by surface topography and surface and near surface damages such as burns and micro and macro-cracking induced by phase transformations and residual stresses. The complex force interaction between the grinding wheel and the workpiece results in temperature rise ultimately bringing changes in microstructure of the workpiece under critical temperature histories. For instance, phase transformation may be initiated by austenizing and quenching of steel as occurred in ground components. These types of damage may reduce the life of critical components that are often subjected to severe working conditions with repeated loading and vibrations. The complexity of grinding process indicates that much attention should be paid to the modelling of phase transformation kinetics and their consequences on the thermo-mechanical behaviour of the material in

addition to thermal modelling, mechanical modelling and modelling for the contact mechanism of the grinding process [1]. In the present work an effort is made to model phase transformation kinetics in a very simplified manner which is readily available for use as FORTRAN subroutine.

2.0 METHODOLOGY

2.1 Phase Transformations Models

Different approaches for modelling phase transformations in various machining processes have been discussed in [2]. In this study the approach based on the material's time-temperature transformation behaviour, earlier proposed by Johnson and Mehl [3], then Avrami [4-5], in order to predict the evolution of the phase proportions was adopted. In this approach austenitization temperature is described in relation to the thermal activation. It was supposed that the pearlite appears through nucleation then growth, depending on austenite. If the mechanisms are different, other models proposed in [6, 7] may be used for the transformation of ferrite and bainite. The equation of Johnson-Mehl-Avrami is written for isothermal transformation, whereas the demand in calculation comes mainly from anisothermal processes like heat treatment etc. That's why some authors proposed

modifications of the preceding model to take into account anisothermal effects, see Inoue [8] and further models by [9-11].

The martensitic transformations are treated separately, because considered as independent of time. The empirical law of Koistinen and Marburger [12] gives the volume fraction of martensite according to the temperature. Leblond [13, 14] proposed a model based on a law of simplified evolution utilizing a proportion of transformed phase in equilibrium and a constant of time without employing evolution-type equations that necessarily combine martensite growth and transformation plasticity.

Waeckel [15] also proposed a model with easily identifiable parameters starting from CCT diagram and able to reproduce thermal histories of welding. The second order differential equation (CONT) model proposed by [16] may be used for simulations of the problems where additivity rule is not required.

2.2 Proposed Model For Transformation

In case of diffusion-controlled transformations, the metallurgical transformation kinetics during a heating/continuous cooling process is determined using the isothermal transformation kinetics for the material studied. The transformed fraction of phase *i*, z_i is calculated based on the Avrami [4] type model designed to compute phase transformation kinetics during heating and cooling. The proposed model is expressed as:

$$z_i = z_i^{eq} \left[1 - \exp \left\{ -\kappa_i(T) \cdot (t)^{m_i(T)} \right\} \right] \quad (1)$$

where z_i is the average phase fraction of constituent *i* at time *t* and z_i^{eq} is the equilibrium (or maximum)

fraction of phase *i* while κ_i and m_i are empirically obtained constants for the phase *i*. according to Christian [17], the suggested value for m_i may range between 1 and 4.

The Avrami [5] equation was originally proposed for an isothermal condition, for non-isothermal transformation kinetics, the additivity rule by Scheil [18] was applied where the temperature-time curve is discretized in a series of isothermal steps. On each step the volume fraction of new phase formed is calculated by using isothermal transformation kinetics. The principle of transition from isothermal step *n* to next step *n+1* is based on the introduction of an equivalent time t_o for each transformation, as illustrated in Figure 1. z_i is the proportion of austenite formed at the end of step *n*. At the beginning of step *n+1*, the phase proportion z_i allows to determine the equivalent time t_o from isothermal kinetics defined for the step *n+1*.

$$z_{i,n+1} = z_{i,n+1}^{eq} \left[1 - \exp \left\{ -\kappa_i(T) \cdot (t_o + \Delta t)^{m_i(T)} \right\} \right] \quad (2)$$

$$t_o = \left(-\frac{1}{\kappa_i} \ln \left(1 - \frac{z_{i,n}}{z_i^{eq}} \right) \right)^{\frac{1}{m_i}} \quad (3)$$

The parameters $\kappa_i(T)$ and $m_i(T)$ are obtained as follows:

The coefficients $\kappa_i(T)$ and $m_i(T)$ are calculated at each temperature from the transformation curves of a continuous cooling transformation (CCT) diagram by assuming that it gives the start time t_S when a small proportion (e.g. 1%) of the new phase is formed and the end time t_E when 99% of the equilibrium phase fraction z_i^{eq} is formed at constant temperature *T*

$$\left. \begin{aligned} 1 - \exp \left\{ -\kappa_i(T) \cdot (t_S)^{m_i(T)} \right\} &= 0.01 \\ 1 - \exp \left\{ -\kappa_i(T) \cdot (t_E)^{m_i(T)} \right\} &= 0.99 z_i^{eq} \end{aligned} \right\} \quad (4)$$

The transformation parameters $\kappa_{i(T)}$ and $m_{i(T)}$ are obtained by solving eq. (3):

$$\kappa_i(T) = -\frac{1}{(t_E)^{m_i(T)}} \ln(1 - 0.99 z_i^{eq}) \quad (5)$$

$$m_i(T) = \frac{1}{\ln \left(\frac{t_S}{t_E} \right)} \ln \left[\frac{\ln(1 - 0.01)}{\ln(1 - 0.99 z_i^{eq})} \right] \quad (6)$$

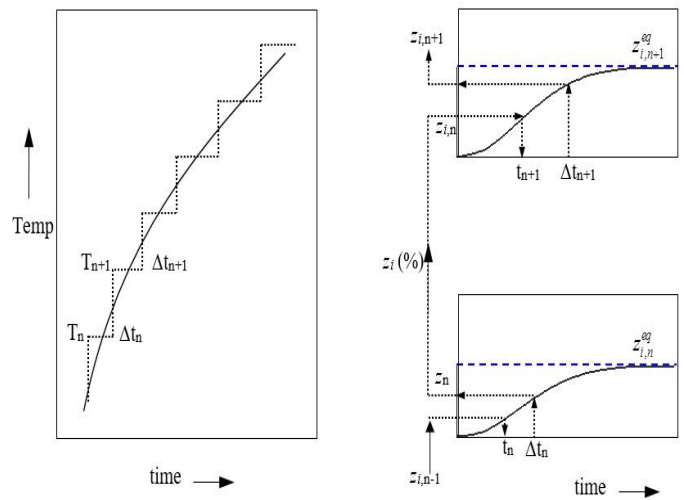


Figure 1 Schematic representation of computation of new phase formed

The metallurgical history of a point depends mainly on its thermal history. This dependency is described by a CCT diagram that gives the start and end of transformation temperatures, either according to cooling rate, or according to cooling time. For the metallurgical evolution of the material i.e. the phase proportion evolution is determined using the equations proposed in the subsequent paragraph. The CCT diagrams obtained experimentally for AISI 52100 steel in the work of various researchers will be used to determine model parameters. This is done by aligning the data of the CCT diagram of AISI 52100 steel as closely as possible with the predictions provided by the suggested models. This identification consequently involves executing successive tests with the numerical model for different parameters, then selecting those which provide results comparable with those of the experimental diagrams.

2.3 Heating

For heating process the model is based on the knowledge of the Isothermal Transformation diagram during heating. For example, the material under investigation (AISI 52100 / 100Cr6 steel) is a hypereutectoid carbon steel with a carbon content $C > 0.8$ (Figure 2) and an initial ferrite-cementite structure. The time-temperature-austenitization (TTA) diagram taken for the model is shown in Figure 3.

The Austenite appears instantaneously from the pearlite, between temperatures Ac_1 and Ac_3 , until complete dissolution of pearlite has occurred (curve 1, Figure 3). The percentage of austenite formed z^{eq} can be determined from CCT diagram (Figure 7). The end of transformation is defined by curve 2 in Figure 3. Above the temperature Ac_3 , curve 2 represents the time required for the complete dissolution of both pearlite and ferrite. After this time the structure is totally austenitic.

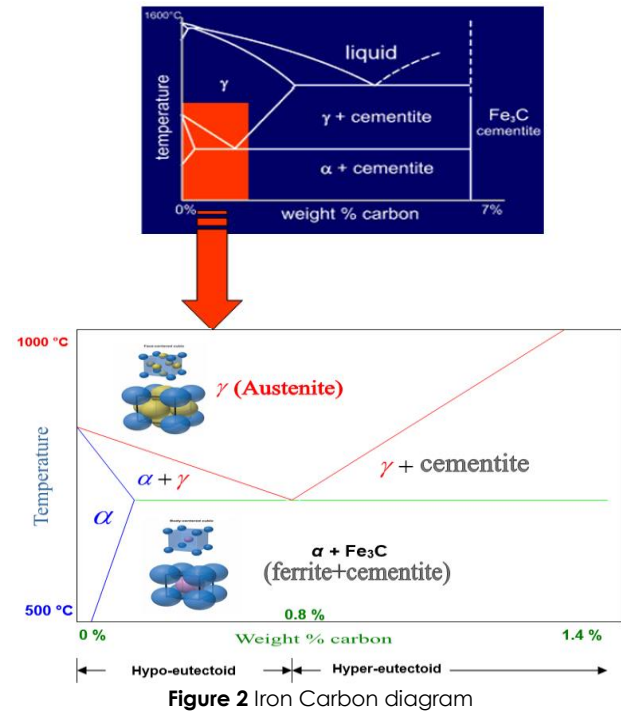


Figure 2 Iron Carbon diagram

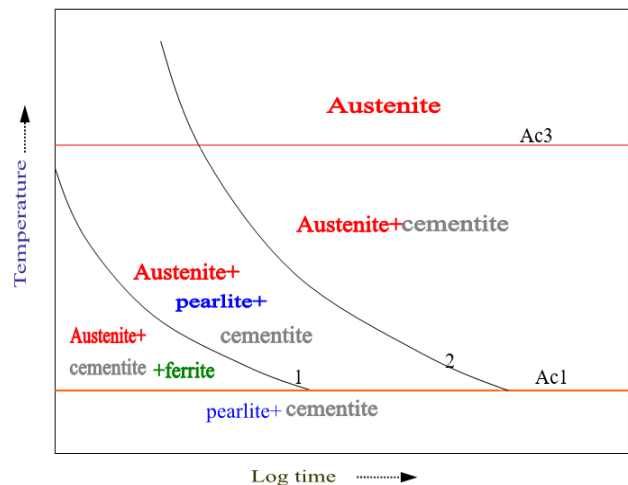


Figure 3 Isothermal Transformation diagram for a hyper-eutectoid steel (for heating) [19]

2.4 Cooling

After heating to an austenitizing temperature, cooling has to take place at various cooling rates to allow the material transformation into different phases. The carbon atoms previously dissolved in the austenite remain in their interstitial lattice positions and distort the corresponding body-centred cubic lattice into different lattice structures, depending mainly upon cooling rate and temperature. If the transformation process proceeds slowly (slow cooling rate), carbon has the opportunity to diffuse more or less into the iron lattice. This is called a diffusion

controlled transformation. If the transformation process proceeds rapidly (high cooling rate), the face-centred cubic iron lattice shears without diffusion into a face-centred cubic iron lattice, the dissolved carbon is 'captured' in the iron lattice and distorts the body centred lattice tetragonal; as it forms. The material so produced is termed martensite (hard). This is called a diffusionless transformation through shearing.

For the phase transformation calculations during cooling, the model used is based on the knowledge of continuous cooling transformation (CCT) diagram for the steel (AISI 52100 steel), as illustrated in Figure 6. For diffusion-dependent phase transformation calculations (pearlite, bainite), equation 1 is used, while for the diffusionless transformation calculations (martensitic transformation) which do not depend directly on time but only on temperature, the Koistinen-Marburger [13] equation is used:

$$z_M = z_y \{1 - \exp[-\beta(M_s - T)]\} \quad (7)$$

Where z_M and z_y are martensitic and austenitic phase proportions, respectively, β is a material constant typically chosen in the order of 0.01 for plain carbon steel. M_s is the temperature at which the martensitic transformation starts, and T the temperature.

2.5 Numerical Implementation

The numerical implementation of the proposed model was carried out through a FORTRAN subroutine called PHASE using the FEM commercial software Abaqus®/standard. A series of FEM simulations were performed for a 2D single element (0.001×0.001 m²) being the optimal size to save computing time. The element type CPE4T (4-node plane strain thermally coupled quadrilateral bilinear displacement and temperature) was used for the analysis (Figure 4).

2.6 Initial Conditions, Assumptions and Boundary Conditions

It was assumed that heating is uniform and the maximum temperature is sufficient to initiate austenite phase transformation. The component can therefore be assumed to be stress-free and 100% austenitic. The simulation starts with no stress at an initial temperature and above A_{c3} with 100% austenite. The cooling characteristics in relation to phase transformations are given by the CCT diagram. The martensitic start temperature is given by M_s and the final temperature is the ambient one. Other critical transformation temperatures are given by P_s (pearlitic start temperature) and B_s (bainitic start temperature). Four metallurgical phases are assumed for the simulation: austenite, pearlite, bainite, and martensite.

The initial temperature was set to 20°C. A convective heat transfer was applied at the walls. The thermal and mechanical boundary conditions are shown in Figure 4.

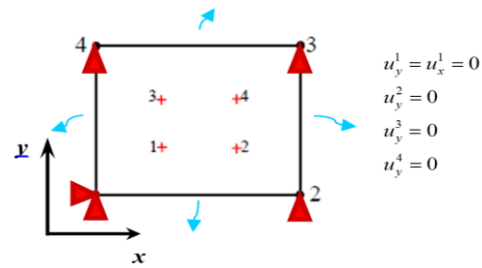


Figure 4 Mechanical and thermal boundary conditions for the single element analysis

The material used was AISI 52100 (100Cr6) steel. The chemical composition of the material is given in Table 1.

Table 1 Chemical composition of AISI 52100 (100Cr6) bearing steel

	0.95	0.15	0.20		1.35		
Mass %	to	to	to	≤0.025	to	≤0.10	≤0.030
	1.10	0.35	0.40		1.60		

The analysis was performed in two steps. The element was first heated to 1000°C at a constant heating rate and then cooled down to room temperature at different cooling rates. The different temperature histories used are shown in Figure 5. During cooling the heat source was removed and convective cooling was applied to all four sides of the specimen. The phase transformation calculations are done with the subroutine PHASE. Micro-structural constituents are defined as state variables. They are computed and updated inside the subroutine PHASE.

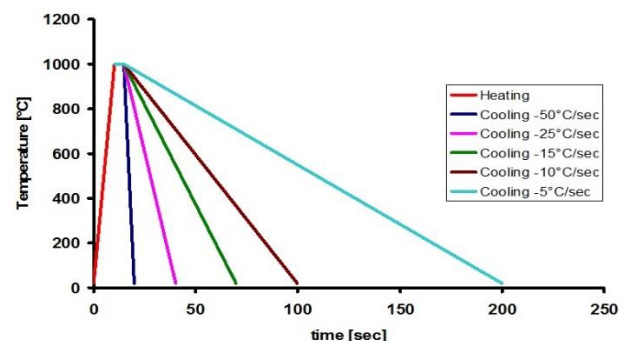


Figure 5 Different temperature histories used

3.0 RESULTS AND DISCUSSION

Figure 6 shows the CCT diagram for the material AISI 52100 (100Cr6) steel, which has been divided in four regions according to the number of transformations that may occur during cooling. The phase transformation calculations are performed according to the cooling rate lines falling in the specified regions. For instance Region 1 corresponds to slow cooling rate where the only phase formed is pearlite due to very slow cooling rates. Regions 2 and 3 correspond to medium cooling rates where more than one phase (pearlite, bainite and martensite) may be formed. In Region 4 high cooling rate leads to the formation of martensite.

Two factors are important while determining the transformation products during a cooling process as result of transformation emerging from austenite, the cooling rate (from the CCT diagram, see Figure 6) and the temperatures (T_s and T_f), that lead to transformation. For a specific product i , there is a lower critical cooling rate \dot{T}_L^i , and an upper critical cooling rate, \dot{T}_U^i (Figure 6) within which it is formed during cooling. For this case only pearlite phase may be formed within a cooling rate $< 8 \text{ K.s}^{-1}$ ($-265 \text{ }^\circ\text{C.s}^{-1}$) and an overall cooling rate ranging between $\dot{T}_L^P \approx 0 \text{ K s}^{-1}$ ($-273 \text{ }^\circ\text{C.s}^{-1}$) and $\dot{T}_U^P \approx 40 \text{ K.s}^{-1}$ ($-233 \text{ }^\circ\text{C.s}^{-1}$). The bainitic transformations occur within the range of cooling rate from $\dot{T}_L^B \approx 8 \text{ K.s}^{-1}$ ($-265 \text{ }^\circ\text{C.s}^{-1}$) and $\dot{T}_U^B \approx 40 \text{ K.s}^{-1}$ ($-233 \text{ }^\circ\text{C.s}^{-1}$), and the martensite transformations in the cooling rate range between $\dot{T}_L^M \approx 23 \text{ K.s}^{-1}$ ($-250 \text{ }^\circ\text{C.s}^{-1}$) and $\dot{T}_U^M \approx 40 \text{ K.s}^{-1}$ ($-233 \text{ }^\circ\text{C.s}^{-1}$). Similarly we may have combined pearlitic-bainitic-martensitic transformations in the cooling rate range from $\dot{T}_L^{PBM} \approx 8 \text{ K.s}^{-1}$ ($-265 \text{ }^\circ\text{C.s}^{-1}$) to $\dot{T}_U^{PBM} \approx 22 \text{ K.s}^{-1}$ ($-251 \text{ }^\circ\text{C.s}^{-1}$), and bainitic-martensitic transformations between $\dot{T}_L^{BM} \approx 23 \text{ K.s}^{-1}$ ($-250 \text{ }^\circ\text{C.s}^{-1}$) and $\dot{T}_U^{BM} \approx 40 \text{ K.s}^{-1}$ ($-265 \text{ }^\circ\text{C.s}^{-1}$).

Figures 7 (a, b, c & d) show the phase transformation calculations from initial ferrite state to austenite during heating for constant heating rate, and austenite to pearlite, bainite and martensite phases during cooling according to different cooling rates. Similarly the evolutions of different phase fractions with cooling rate are shown in Figures 8 (a, b & c).

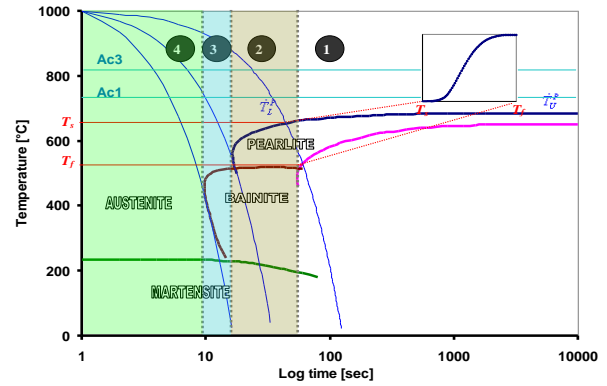
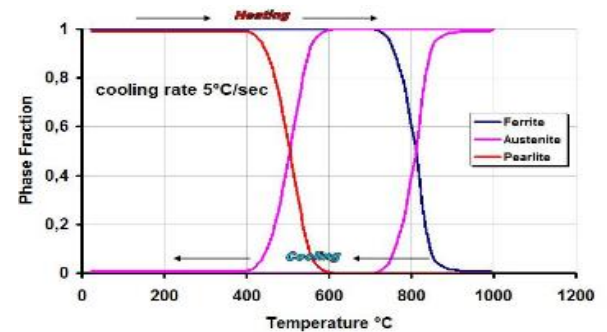
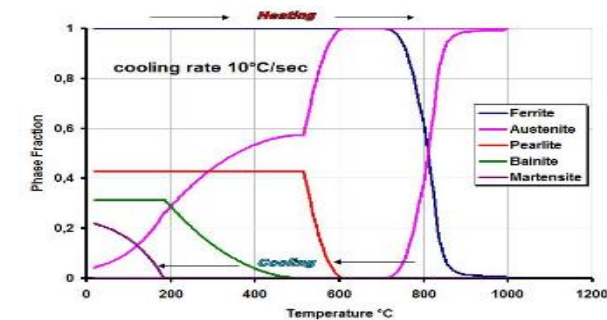


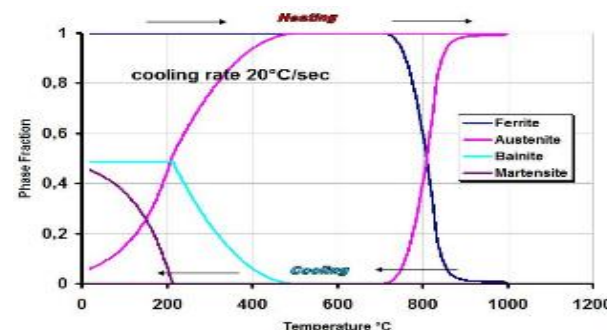
Figure 6 CCT diagram of AISI 52100 steel showing regions of possible phase transformations according to different cooling rates



(a)



(b)



(c)

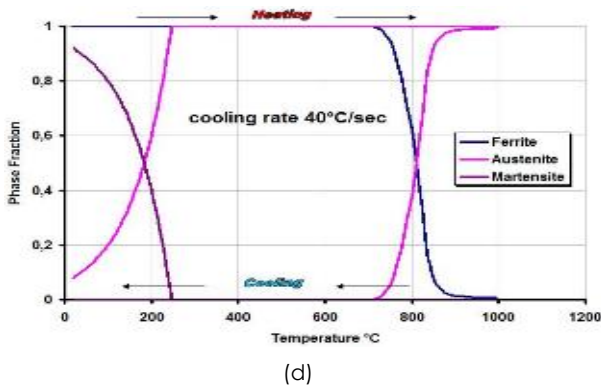


Figure 7 Evolution of phases at different cooling rates

The transformation products for a complete heating and slow cooling cycle are shown in Figure 7 (a), only pearlitic phase transformation has occurred due to a slow cooling rate ($\dot{T} = 5 \text{ K.s}^{-1}$), which corresponds to region-1 in Figure 6. The combined transformation of pearlite, bainite and martensite phases from austenite at a cooling rate $\dot{T} = 10 \text{ K.s}^{-1}$ is presented in Figure 7 (b) (region-2 in Figure 6). Figure 7 (c) shows transformation of bainite and martensite from austenite at a cooling rate of 20 K.s^{-1} , it may be observed that no more pearlite has been transformed as for region 3 in Figure 6. Figure 7 (d) shows that austenite has directly converted into martensite due to the high cooling rate (40 K.s^{-1}) corresponding to region 4 in Figure 6.

The predicted percentages of different individual phases transformed at different cooling rates are presented in Figures 8 (a, b & c). Figure 8 (a) describes the evolution and percentage of the residual pearlite phase at the end of the cooling process for different cooling rates. At low cooling rates we can have high percentage of pearlite phase when the material is heated and cooled to ambient temperature. The formation of pearlite can be suppressed or completely eliminated by using higher cooling rates. The formation of individual bainite phase is shown in Figure 8 (b) which normally appears at medium cooling rates. In contrast to pearlite phase, bainite has low or zero percent content at slow and high cooling rates. Similarly the evolution and percentage of martensite is described in Figure 8 (c). At high cooling rates a maximum content of martensite is observed.

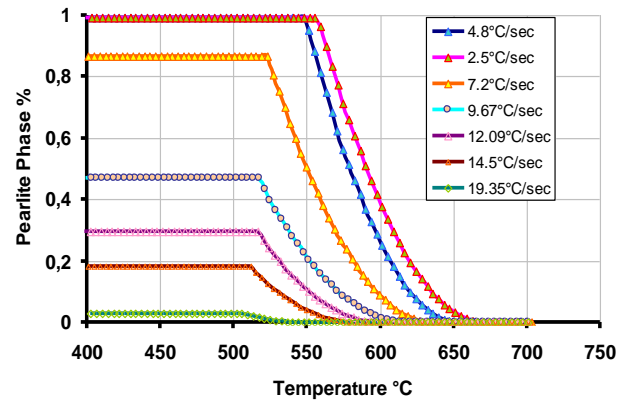


Figure 8 (a) Predicted evolution and phase fraction of Pearlite for different temperature histories

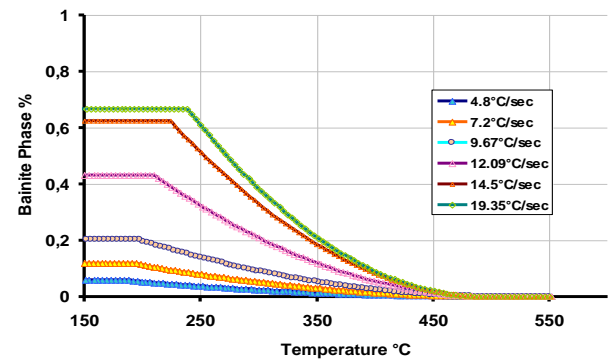


Figure 8 (b) Predicted evolution and phase fraction of bainite for different temperature histories

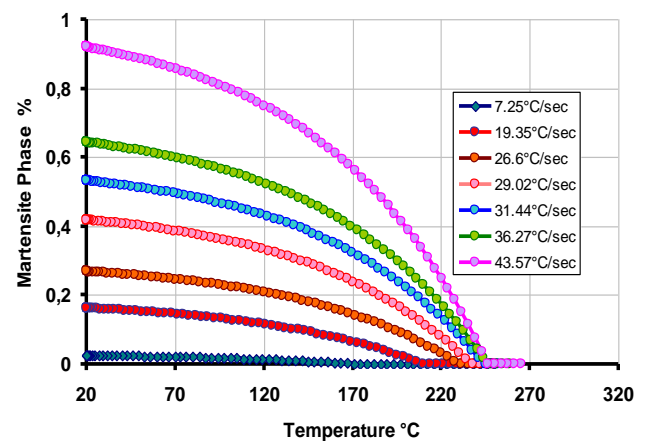


Figure 8 (c) Predicted evolution and phase fraction of martensite for different temperature histories

The overall transformation mechanism of the material AISI 52100 (100Cr6) steel for different cooling rates is presented in Figure 9 (a). The percentage of phases that can be obtained with respect to time, required to cool the material to the ambient temperature is shown in Figure 9 (b). The results of the

simulated phase transformations for the material AISI 52100 (100Cr6 steel) are compared with experimental results of Wever [20] and simulated results of Hunkel [21] (Figure 10) and have been found in a very good agreement.

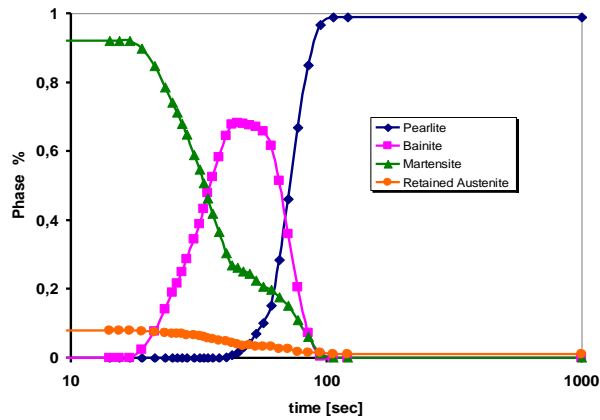


Figure 9 (a) Prediction of volume fraction versus cooling rate for AISI 52100 (100 Cr6) steel

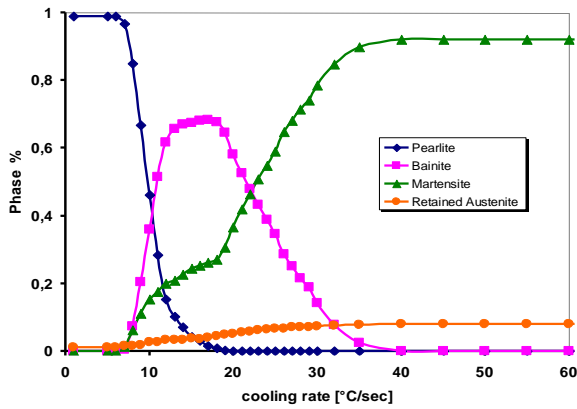


Figure 9 (b) Prediction of volume fraction versus time for AISI 52100 (100 Cr6) steel

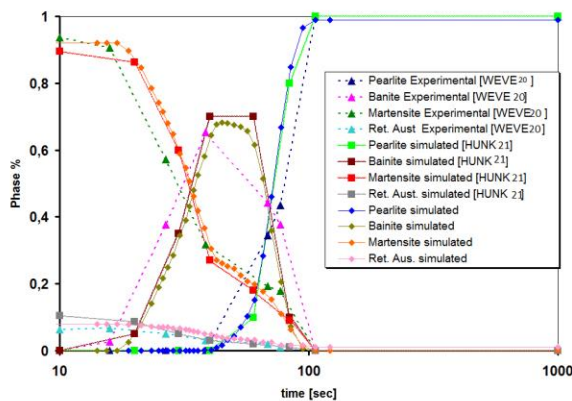


Figure 10 Comparison of simulated and experimental results of phase proportions for AISI 52100 steel

The transformation temperature, T_t (including T_s and T_f), can directly be plotted against the cooling rate \dot{T} creating a T_t - \dot{T} diagram **Figure 11**. A T_t - \dot{T} diagram which is equivalent to a CCT diagram in terms of the continuous cooling transformation kinetics. For the CCT diagram under discussion it can be shown that M_s and B_s , are almost independent of \dot{T} in most of the \dot{T} range but the percentage of the phase fractions of bainite and martensite formed are dependent of the cooling rate.

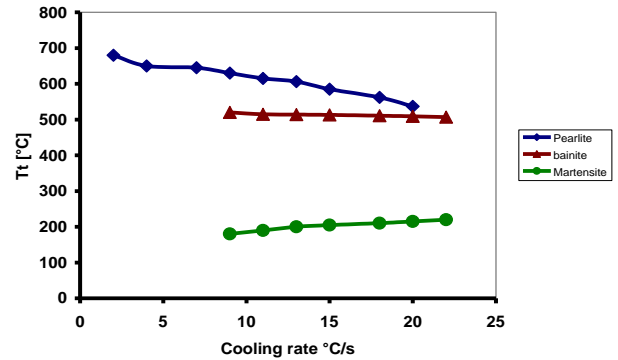


Figure 11 T_t - \dot{T} diagram (cooling rate diagram and Transformation temperature)

4.0 CONCLUSION

A model for phase transformation as occurred during grinding process was proposed and based on that model a FORTRAN subroutine was developed and named PHASE. The numerical implementation of the model was carried out through the developed subroutine using the FEM commercial package Abaqus®/standard. A series of FEM simulations were performed for a single 2D element. Phase transformations were simulated for different thermal histories and the results compared to those in the literature. The predicted percentages of different individual phases transformed at different cooling rates are presented. It was shown that at low cooling rates high percentage of pearlite phase is obtained when the material is heated and cooled to ambient temperature. Bainite is formed usually at medium cooling rates. Similarly at high cooling rates maximum content of martensite may be observed.

The results of the simulated phase transformations for the material AISI 52100 (100Cr6 steel) are compared with experimental results in the literature and were found in a very good agreement.

Nomenclature

Symbol	Units	Significance	Symbol	Units	Significance
α_α	-	thermal expansion coefficient of alpha phase	T_f	[°C]	Transformation finish temperature for a phase constituent
α_γ	-	thermal expansion coefficient of gamma phase	\dot{T}_L^i	[°C]	Lower critical cooling rate of phase i
β	-	material constant	\dot{T}_U^i	[°C]	Upper critical cooling rate of phase i
ϵ_α^{th}	-	thermal strain of alpha phase	\dot{T}	[°C/se c]	Cooling rate
ϵ_γ^{th}	-	thermal strain of gamma phase	T_{auc}	[°C]	Austenizing temperature
$\Delta\epsilon_{\alpha\gamma}^{25^\circ C}$	-	thermal strain difference between two phases	t_o	[sec]	Equivalent transformation time
C_{z_i}	[N/m ²]	Strength multiplier of the phase i	t_s	[sec]	Time when an assumed small portion of phase has transformed
κ_i	-	Empirically obtained constant for the phase i	t_e	[sec]	Time when assumed equivalent proportion of phase has transformed
M_s	[°C]	martensite start temperature	z		Phase fraction
n_i	-	Empirically obtained constant for the phase i	z_i		Average phase fraction of constituent i
σ_y^α	[N/m ²]	Yield stress of alpha (ferrite) phase	z_i^{eq}		Equilibrium fraction of phase i that is achieved after an infinite long time
σ_y^γ	[N/m ²]	Yield stress of gamma (austenite) phase	z_γ		Austenite phase fraction
T_s	[°C]	Transformation start temperature for a phase constituent	z_M		Martensite phase fraction

Acknowledgement

The authors wish to thank Balochistan University of Engineering and Technology Khuzdar, Pakistan for providing access to their equipment and technical support of their staff

References

- [1] Shah S. M. A., D. Nelais, M. Zain, M. Coref. 2012. Numerical Simulation of Grinding Induced Phase Transformation and Residual Stresses in AISI-52100 Steel. *International Journal of Finite Elements in Analysis and Design*. 61: 1-11.
- [2] Schulze, V., Uhlmann, E., Mahnken, R., Menzel, A., Biermann, D., Zabel, A., & Bartel, T. 2015. Evaluation of Different Approaches for Modeling Phase Transformations in Machining Simulation. *Production Engineering*. 9(4): 437-449.
- [3] Johnson, W. A., & Mehl, R. F. 1939. Reaction Kinetics in Processes of Nucleation and Growth. *Trans. Aime*. 135(8): 396-415.
- [4] Avrami, M. 1939. Kinetics of Phase Change. I General Theory. *The Journal of Chemical Physics*. 7(12): 1103-1112.
- [5] Avrami, M. 1940. Kinetics of Phase Change. II Transformation-time Relations for Random Distribution of Nuclei. *The Journal of Chemical Physics*. 8(2): 212-224.
- [6] Bhadeshia, H. K. D. H. 2001. *Bainite in Steels*. The Inst. of Meter. 2nd Ed. Institute of Materials.
- [7] Webster, G. A., and Ezeilo, A. N. 2001. Residual Stress Distributions and Their Influence on Fatigue Lifetimes. *International Journal of Fatigue*. 23(1): 375-383.
- [8] Inoue, T. and Raniecki, B. 1978. Determination of Thermal-hardening Stress in Steels by Use of Thermoplasticity Theory. *Journal of the Mechanics and Physics of Solids*. 26(3): 187-212.
- [9] Habraken, A. M. and Bourdouxhe, M. 1992. Coupled Thermo-mechanical-metallurgical Analysis During the Cooling Process of Steel Pieces. *European Journal of Mechanics. A. Solids*. 11(3): 381-402.
- [10] Sjöström, S. 1985. Interactions and Constitutive Models for Calculating Quench Stresses in Steel. *Materials Science and Technology*. 1(10): 823-829.
- [11] Fernandes, F. M. B., Denis, S. and Simon, A. 1985. Mathematical Model Coupling Phase Transformation and Temperature Evolution During Quenching of Steels. *Materials Science and Technology*. 1(10): 838-844.
- [12] Koistinen, D. P. and Marburger, R. E. 1959. A General Equation Prescribing the Extent of the Austenite-Martensite Transformation in Pure Iron-carbon Alloys and Plain Carbon Steels. *Acta Metallurgica*. 7(1): 59-60.
- [13] Leblond, J. B. and Devaux, J. 1984. A New Kinetic Model for Anisothermal Metallurgical Transformations in Steels Including Effect of Austenite Grain Size. *Acta Metallurgica*. 32(1): 137-146.
- [14] Leblond, J. B., Mottet, G., Devaux, J. and Devaux, J. C. 1985. Mathematical Models of Anisothermal Phase Transformations in Steels, and Predicted Plastic Behaviour. *Materials Science and Technology*. 1(10): 815-822.
- [15] Waeckel, F., Dupas, P. and Andrieux, S. 1996. A Thermo-Metallurgical Model for Steel Cooling Behaviour: Proposition, Validation and Comparison with the Sysweld's Model. *Le Journal de Physique IV*. 6(C1): C1-255.
- [16] Wroźyna, A., Pernach, M., Kuziak, R. et al. 2016. Experimental and Numerical Simulations of Phase Transformations Occurring During Continuous Annealing of Dp Steel Strips. *Journal of Material Engineering and Performance*. 25: 1481.
- [17] Christian, J. W. 2002. *The Theory of Transformations in Metals and Alloys*. PERGAMON. An Imprint of Elsevier Science.
- [18] Scheil, E. 1935. Start-up Time of Austenitic Conversion. *Archive for the Ironworks*. 12: 564-567.
- [19] Owaku, S., and Akasu, H. 1963. Time-Temperature-Austenitization Diagram of Hypereutectoid Steel. *Transactions of the Japan Institute of Metals*. 4(3): 173-178.
- [20] Wever, F. A. Rose, W. Peter, W. Strassburg and L. Rademacher. 1959. *Atlas for the Heat Treatment of Steels*. Verlag Stahleisen, GmbH, Germany.
- [21] Hunkel, M., Lübben, T., Hoffmann, F. and Mayr, P. 2004. Using the Jominy End-quench Test for Validation of Thermo-metallurgical Model Parameters. *Journal de Physique IV*. 120: 571-579.